Korean J. Chem. Eng., 34(8), 2169-2179 (2017)
DOI: 10.1007/s11814-017-0113-2

pISSN: 0256-1115
eISSN: 1975-7220

Multifunctional human-hair nanocomposites for oxidation of alcohols, *aza*-Michael reactions and reduction of 2-nitrophenol

Mayakrishnan Gopiraman and Ill-Min Chung†

Department of Applied Bioscience, College of Life & Environment Science, Konkuk University,
120, Neungdong-ro, Gwangjin-gu, Seoul 05029, Korea
(*Received 24 February 2017 • accepted 12 April 2017*)

Abstract−Novel nanocatalysts (Ni/HHP and Ru/HHP) were prepared by a very simple chemical reduction method. Fine human hair powder (HHp) was obtained from raw human hair (HH) by ball milling method. Readily leachable constituents were removed from HHp to obtain HHP. The HHP was employed as support for the decoration Ni and Ru nanoparticles (NPs). Strong interaction between ultrafine NPs and HHP was revealed. Weight percentage of Ru in Ru/HHP and Ni in Ni/HHP was determined to be 39.65% and 26.36%, respectively. Chemical state of nanocatalysts was studied by XPS and XRD analyses. Merit of Ru/HHP and Ni/HHP was realized from its excellent catalytic activity. The Ru/HHP and Ni/HHP worked well for the oxidation and *aza*-Michael reactions, respectively. Moreover, both Ni/HHP and Ru/HHP were found to be excellent for the reduction of 2-nitrophenol (2-NP). Reusability, stability and heterogeneity of the catalysts were demonstrated. A mechanism has been proposed for catalytic systems.

Keywords: Human Hair, Nanoparticles, Immobilization, Green Composites, Catalysis

INTRODUCTION

Metal nanoparticles (MNPs)-mediated organic transformations are very important reactions in pharmaceuticals and fine chemicals [1]. However, aggregation of MNPs is unavoidable in the absence of any supports, which leads to their low catalytic activity as well as poor reusability [2]. To date, numerous supports including γ-Al_2O_3 [3], silica [4], ceria [5], boehmite [6], aluminosilicates [7], carbonaceous materials [8], Zeolites [9] and polymeric materials [10] have been employed to stabilize catalytic MNPs. Generally, supported-MNPs catalysts were found to be better due to high surface area and fine dispersion. Zhuang et al. [11] prepared Ni-supported nitrogen-doped carbon nanotubes and utilized them as hydrogen oxidation reaction catalyst in alkaline electrolyte. Guard et al. reported Ni precatalysts for the Suzuki-Miyaura reaction [12]. Similarly, there are several supported-MNPs catalysts including CuO/MWCNT [8], Ru/GNS [13], CuO/GNS [14], RuO_2/SWCNT [15], RuO_2NPs/GNPs [16], RuO_2/MWCNTs [17], RuO_2NRs/GNPs [18], Au-Ag/graphene [19], and TiO_2/*u*-RuO_2/GNS [20] reported to date by our research group. Prior to utilizing carbon materials such as CNTs, graphene and CNFs, surface medication is necessary [8,10,13-20]. To control environmental pollution, green materials including cellulose derivatives [21], keratine [22], gram positive and gram-negative bacteria [23], chitosan [24], and mycelial [25] have also been used as supports. In addition, several green plant extracts are employed to prepare environmentally friendly catalysts for various applications [26-28]. Despite that, most of the supports are expensive, difficult to fabricate and often require surface modification to make them suitable for the decoration of MNPs. Recently, cellulose nanofibers-based MNPs catalysts were reported in which the surface of the nanofibers is modified with anionic groups [10]. In addition, higher metal loading is also limited. Hence there has been a continuous search for cheap and green support for the preparation of efficient nanocatalysts.

Human hair (HH) is largely abandoned but often is considered to be a biowaste material [29]. HH contains 88% of keratin and the remaining is proteins, lipids, water, trace elements and pigments. The keratin is very hard, stable and insoluble fibrous structural proteins in most of the organic solvents [30]. Inspiringly, HH is easily available, bio-degradable and cost effective biomaterial. Unlike other biowaste materials, the HH has various electron donors (S, N, P and O) in fibrous, which can assist HH to have a strong interaction with MNPs *via* charge transfer between MNPs and HH. The HH composites are utilized in biomedical applications [31]. Moreover, the HH has being used as fertilizers and to make ropes for horse riding [29]. Haveli et al. [32] demonstrated a controlled synthesis of fluorescent Ag nanoparticles using human hair fiber as a reactor/medium. Similarly, Walter et al. [33] formed PbS nanocrystals within the HH-matrix during blacking. They found that the shape and distribution of nanoparticles are controllable. Very recently, we proved that human hair can be a suitable support for the decoration of Ag and Au NPs [34], and the obtained nanocatalysts are highly efficient, heterogeneous and reusable towards cyclo addition and *aza*-Michael reactions, respectively. Based on these points, we presumed that the HH would be suitable for immobilization of Ni and Ru NPs. In this study, HH was used as support for the decoration of Ni NPs and Ru NPs. The resultant Ni/HHP and Ru/HHP composites were completely characterized by means of SEM-EDS, TEM, XPS, XRD and BET analysis. The nanocomposites were tested as catalysts for *aza*-Michael reaction and oxidation of alco-

†To whom correspondence should be addressed.
E-mail: imcim@konkuk.ac.kr, illminchung@gmail.com

hols. Further, the Ni/HHP and Ru/HHP were tested as catalysts for the reduction of 2-nitrophenol (2-NP). Reusability and stability were also demonstrated.

EXPERIMENTAL

1. Materials and Characterization

HH was collected from Ueda salon stores in Nagano, Japan. All other chemicals were purchased from Sigma Aldrich or Wako Pure Chemicals and used as received. The morphology of composites was investigated on a JEOL JEM-2100F TEM with accelerating voltage of 120 kV. Imagej software was used to find the size of Ru NPs and Ni NPs; nearly 50 NPs were selected to obtain NPs distribution chart SEM-EDS and corresponding elemental mappings were recorded using Hitachi 3000H SEM. XPS (Kratos Axis-Ultra DLD, Kratos Analytical Ltd., Japan) was recorded to study the chemical state of nanocatalysts. The catalytic activity of composites was studied using Shimadzu-2010 gas chromatograph. ^{13}C NMR (100 MHz) and ^{1}H NMR (400 MHz) spectra were recorded on a Bruker spectrometer. DMSO-d_6 and TMS were used as solvent and internal reference, respectively. See supporting information for more experimental details. Inductively coupled plasma-mass spectrometer (ICP-MS, 7500CS, Agilent) was used to test the heterogeneous and leaching properties of the catalyst. The specific surface area of Ni/HHP and Ru/HHP was calculated by using the Brunauer-Emmett-Teller (BET) method.

2. Preparation of Ni/HHP and Ru/HHP Composites

First, 5.0 g of HH fibers was transformed into fine powder (HHp) by ball milling. Although there may be alternate methods to obtain HHp from HH, the reason for preferring the ball milling method in the present study is very simple and effective. Moreover, the method does not require any additional chemical reagents. The resultant HHp was washed well with water/acetone mixture, and the readily leachable constituents were removed by Shindai method to obtain HHP [35]. In a typical procedure, 3 g of HHp was washed well with ethanol and then stirred in chloroform/methanol mixture (2 : 1, v/v) for 3 days at 50 °C. The resultant residue was further dispersed in aqueous solution (75 mL) containing 25 mM Tris-HCl, 2.6 M thiourea, 5 M urea and 5% 2-mercaptoethanol and magnetically stirred at 50 °C for 24 h. Finally, the mixture was filtered and the resultant solid (HHP) was employed for the decoration of Ni NPs and Ru NPs. The HHP (0.5 g) was dispersed in distilled water (50 mL) containing $NiCl_2$ (0.25 g). Then, the $NiCl_2$ was reduced to Ni NPs by a dropwise addition of 0.25 M of $NaBH_4$ solution. Subsequently, the resultant solution was magnetically stirred at 80 °C for 3 h and then filtered followed by vacuum drying. Similarly, the Ru/HHP was prepared by using $RuCl_3$ (0.1 g).

3. Procedure for Ru/HHP Catalyzed Oxidation of Alcohols

A mixture of Ru/HHP (10 mg), benzyl alcohol (1 mmol) and toluene (3 mL) was magnetically stirred under air atmosphere at 110 °C for 24 h. The completion of the reaction was checked by TLC and GC analyses. After the reaction, the product was isolated and confirmed by NMR analysis. **Benzaldehyde**: ^{1}H NMR (400 MHz, DMSO-d_6): δ 7.65 (m, 5H), 9.99 (s, 1H) ppm; ^{13}C NMR (100 MHz, DMSO-d_6): δ 130.1, 134.9, 137.3, 192.3 ppm.

After the completion of reaction, the Ru/HHP was separated out by centrifugation, and the reaction mixture was analyzed by GC. Samples of both reactants and products were dissolved in toluene and analyzed. GC equipped with 5% diphenyl and 95% dimethyl siloxane, Restek-5 capillary column (0.32 mm dia, 60 m in length), a flame ionization detector (FID) and nitrogen as a carrier gas was used. The initial column temperature was increased from 60 to 150 °C at the rate of 10 °C/min and then to 220 °C at the rate of 40 °C/min. During the product analysis, the temperatures of the FID and injection port were kept constant at 150 and 250 °C, respectively.

Yield of the catalytic product, conversion and selectivity were calculated by using the Eqs. (1), (2) and (3), respectively.

$$\text{GC yield (\%)} = \%\ \text{of product formed} \quad (1)$$

$$\text{GC conversion (\%)} = 100 - \%\ \text{of reactant remains} \quad (2)$$

$$\text{Selectivity (\%)} = 100 - (\text{conversion} - \text{yield}) \quad (3)$$

4. Procedure for Ni/HHP Catalyzed *aza*-Michael Reaction

Acrylonitrile (2 mmol), 1-phenylpiperazine (2 mmol) and Ni/HHP (2 mg) was stirred under air atmosphere at 25 °C for 1 h. The product was isolated using silica column. **3-(4-Phenylpiperazin-1-yl)propanenitrile**: ^{1}H NMR (400 MHz, DMSO-d_6): δ 2.57 (t, 2H), 2.70 (t, 2H), 3.13 (s, 8H), 6.78 (t, 1H), 6.92-6.94 (d, 2H), 7.22 (t, 2H) ppm; ^{13}C NMR (100 MHz, DMSO-d_6): δ 15.3, 48.5, 52.4, 53.0, 115.7, 119.2, 120.3, 129.2, 151.3 ppm.

5. Procedure for Reduction of 2-NP

A mixture of 2-NP (40 μL, 0.01 M), $NaBH_4$ (4 mL, 0.01 M) and catalysts (0.5 or 2.5 mg) was magnetically stirred under open air atmosphere at 25 °C. The reduction of 2-NP was monitored using UV-vis spectroscopy at room temperature. For comparison, the aqueous 2-NP solution (before and after the addition of $NaBH_4$) was also measured. The progress of the reaction was monitored at regular time intervals.

RESULTS AND DISCUSSION

1. Characterization of Ni/HHP and Ru/HHP

HRTEM images were taken for MNPs/HHP (Ni/HHP and Ru/HHP) (Fig. 1). The results confirmed that the NPs were uniformly attached mainly on the surface of HHP. The NPs were spherical and the size of Ni and Ru NPs in MNPs/HHP was found to be extremely small. In fact, such smaller NPs have played significant role in heterogeneous catalysis. The mean diameter of Ni and Ru NPs was calculated to be 4.8 and 5.3 nm, respectively (Figs. 1(c) and 1(d)). Since the average size of Ni and Ru NPs was very small, the surface area per unit mass (S) of Ru and Ni NPs was calculated using the equation $S=6000/(\rho \times d)$, where d is the mean diameter of NPs and ρ is the density of metal [13]. The surface area per unit mass of Ni and Ru NPs was calculated to be 140.3 and 90.9 g cm^{-3}. Generally, the NPs with smaller in diameter often possess several effects including geometric shell closings, electronic shell closings, quantum confinement and superatomic character (electrons are shared among the atoms differently from bulk materials). BET surface area was also determined for the Ni/HHP and Ru/HHP. The human hair powder before MNPs decoration has BET surface area of 53 m^2/g with good pore volume (V_p=0.19 cm^3/g) and average

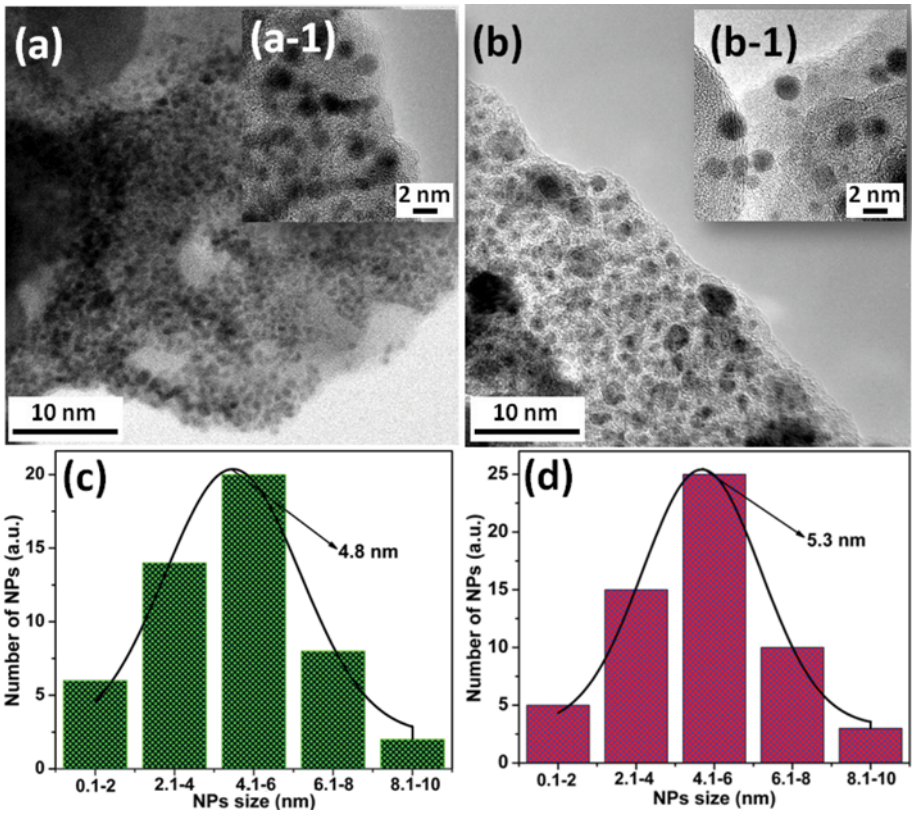

Fig. 1. HRTEM images of (a) Ni/HHP and (b) Ru/HHP; insets (a-1) and (b-1) show the magnified HRTEM images. The histogram of NPs diameter distribution for (c) Ni/HHP and (d) Ru/HHP.

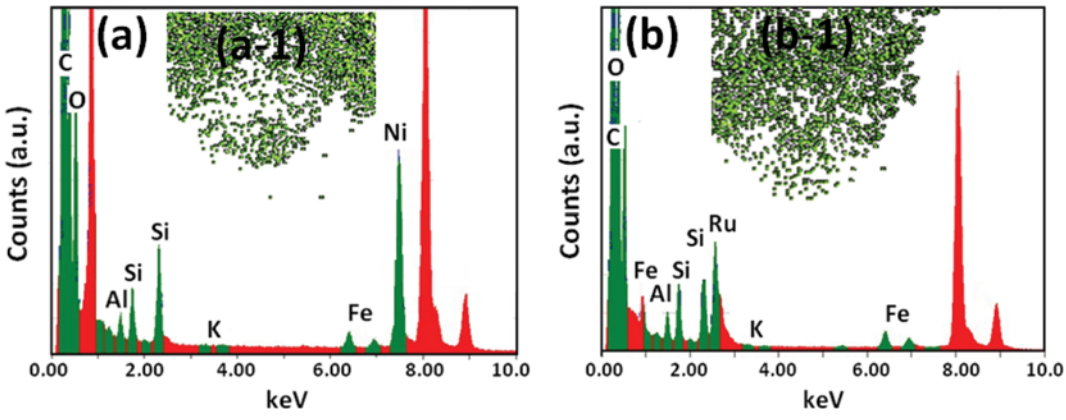

Fig. 2. EDS of (a) Ni/HHP and (b) Ru/HHP; insets show the corresponding elemental mappings of (a-1) Ni and (b-1) Ru.

pore size (dp=14 nm). Siimilarly, Ni/HHP and Ru/HHP were demonstrated a BET surface area of 15 m^2/g (with Vp of 0.11 cm^3/g and dp of 13 nm) and 16 m^2/g (with Vp=0.04 cm^3/g and dp=9 nm), respectively. No leached NPs were seen in the background of HRTEM images, indicating the complete utilization of MNPs. Figs. 1(b) and 1(c) show the EDS spectrum of Ni/HHP and Ru/HHP. The weight percentage of Ni in Ni/HHP and Ru in Ru/HHP was found to be 38.98% and 26.89%, respectively. In addition, other elements such as C, O, Na, Al, Si, S and Fe were also detected. The corresponding elemental mappings for Ni and Ru supported the homogeneous dispersion of MNPs in MNPs/HHP. The better morphology of composites is mainly due to the presence of electron donors (N, P, O and S) in HHP.

SEM and EDS spectra were recorded for Ni/HHP and Ru/HHP to verify the loading of Ni and Ru (Fig. 3). The wt% of Ni and Ru in MNPs/HHP was 40 and 26, respectively. The elemental mapping of MNPs/HHP shows that the distribution of NPs was homogeneous. The loading of NPs on HHP can be controlled. Fig. 3(c) shows the XRD spectra of HHP, Ni/HHP and Ru/HHP. The XRD pattern of HHP showed a broad peak centered at 23° in which two sharp peaks (26.3° and 27.5°) also accommodated. These peaks correspond to hard fibrous keratin [36]. Several new peaks at 38.5°,

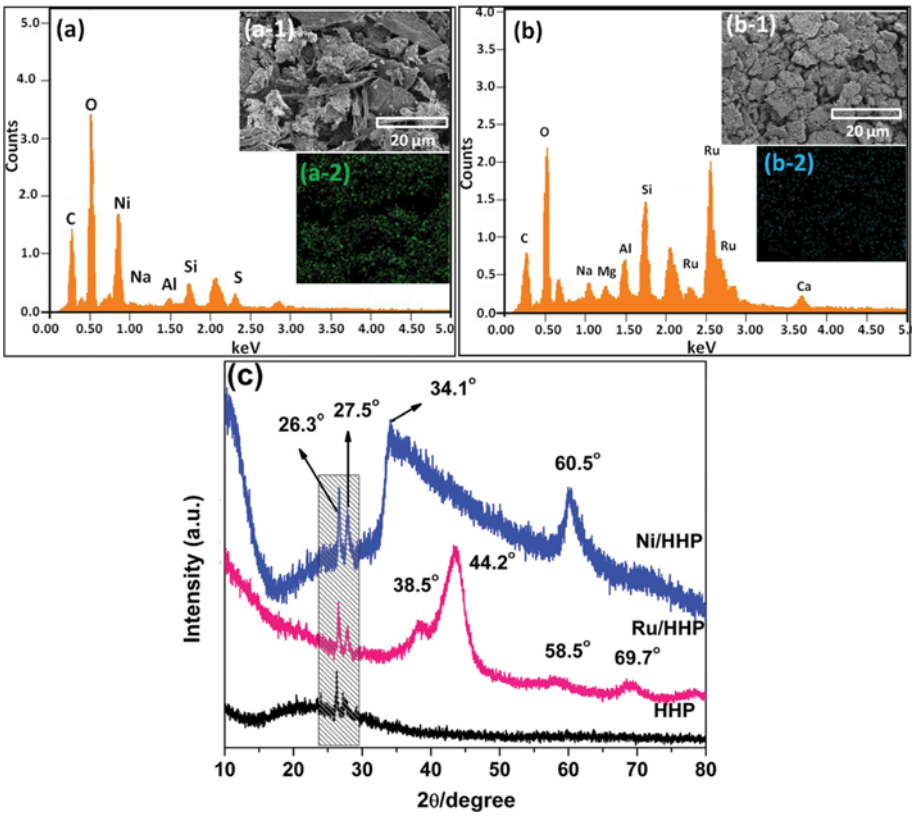

Fig. 3. EDS of (a) Ni/HHP and (b) Ru/HHP; insets show SEM and corresponding mapping of (a-1) and (a-2) Ni/HHP and ((b)- and (b-2)) Ru/HHP. (c) XRD spectra of HHP, Ni/HHP and Ru/HHP.

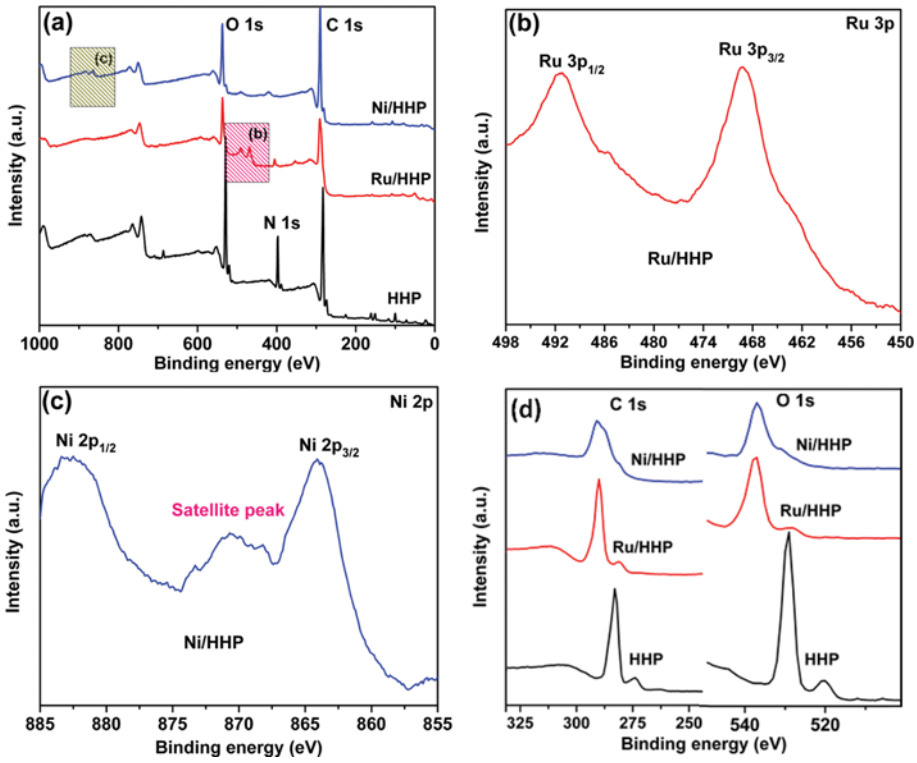

Fig. 4. (a) Survey XPS spectra of HHP, Ru/HHP and Ni/HHP. (b) Ru 3p peaks of Ru/HHP and (c) Ni 2p peaks of Ni/HHP. (d) C 1s and O 1s XPS peaks of HHP, Ru/HHP and Ni/HHP.

44.2°, 58.5° and 69.7° corresponding to metallic Ru were observed for Ru/HHP [37]. Alike, XRD spectrum of Ni/HHP illustrates peaks at 34.1° and 60.5°, indicating the presence of NiO form [38]. The broad peaks confirm the ultrafine nature of NPs which agrees well with HRTEM result.

Fig. 4 demonstrates the XPS spectra of HHP, Ni/HHP and Ru/HHP. All the three samples showed C 1s, O 1s, N 1s and S 1s peaks at 282.8 eV, 529.6 eV, 397.75 eV and 161.6 eV, respectively. For Ru/HHP in Ru 3p region, two new peaks at 463.0 eV (Ru $3p_{3/2}$) and 484.2 eV (Ru $3p_{1/2}$) corresponding to metallic Ru were observed [13]. Similarly, new peaks Ni $2p_{3/2}$ and Ni $2p_{1/2}$ peaks were seen at 864.4 eV and 882.5 eV, respectively [38]. Although the chemical state of Ni and Ru was confirmed by XRD results, the XPS peaks did not match with the previous reports, instead, the peaks dramatically shifted towards higher binding energies. The shift observed in the peaks was obviously due to the excellent adhesion of Ni and Ru NPs with HHP (Fig. 3(d)) [38]. In addition, peaks corresponding to Al, Fe, Si, K and Na were also detected.

2. Ru/HHP Catalyzed Oxidation of Alcohols

2-1. Optimization of Reaction Conditions

Oxidation of alcohols is one of the fundamental reactions in organic chemistry, and the oxidative products are highly useful in various perfume industries [13]. In the present study, Ru/HHP was used as catalyst for the oxidation of alcohols. The reaction conditions such as temperature, time, catalyst amount, atmosphere and solvent were optimized. Oxidation of benzyl alcohol to benzalde-

Table 1. Oxidation of alcohols[a]

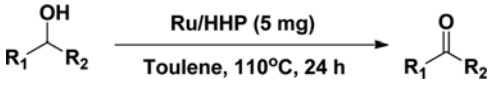

Entry	Substrate	Product	GC data (%)		
			Conversion	Selectivity	Yield
1	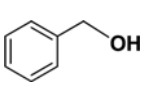	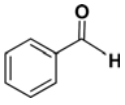	98	100	98
2	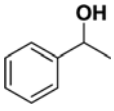	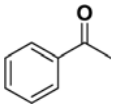	94	100	94
3	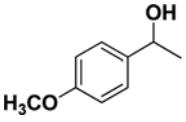	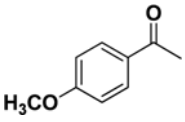	91	94	85
4	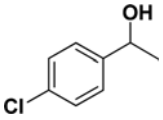	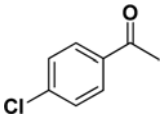	81	98	79
5	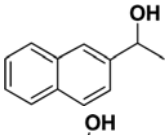	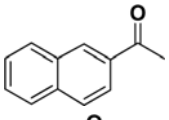	98	100	98
6	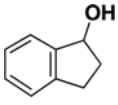	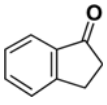	81	88	69
7	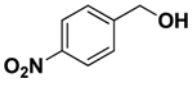	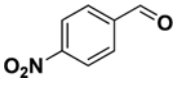	95	96	91
8	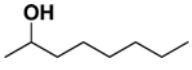	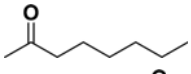	71	100	71
9	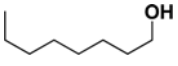	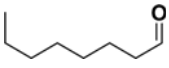	81	98	79
10	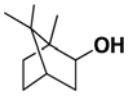	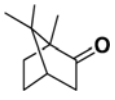	89	80	69
11	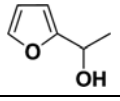	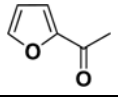	83	78	65

[a]Reaction conditions: Substrate (2 mmol), Ru/HHP (5 mg), toluene (1 mL), 110 °C

hyde was selected as the model reaction. In the absence of Ru/HHP, the reaction gave very poor yield of benzaldehyde. Similarly, the rate of the reaction was slower when the reaction was performed at low temperatures such as 50, 70, 90 and 100°. Better yield of 98% (benzaldehyde) was obtained when the reaction was stirred at 110 °C. In the time optmization, it was found that the reaction was gradually improved with time, and maximum yield was obtained after 24 h. Among different amounts of catalyst taken (2.5 mg and 10 mg), the optimum amount of catalyst was found to be 5 mg. Interestingly, when the reaction was carried out under Ar atmosphere, the system yielded lower yield of 25% of benzaldehyde. Finally, to understand the role of HHP on the yield of benzaldehyde, the pure HHP was used as catalyst; however, the system afforded very low yield of the desired product (~21%). We concluded that the toluene is the best solvent, 110 °C is an optimun temperature, 24 h of reaction time and the optimum amount of Ru/HHP is 5 mg.

2-2. Scope Extension

Further, the scope of the catalytic system was extended. The results (Table 1) show that a wide range of substrates (aliphatic, aromatic, alicyclic, benzylic, allylic, amino and heterocyclic alcohols) can be oxidized to yield the product (Table 1). Under the optimized reaction conditions, the Ru/HHP afforded an excellent yield of 98% (benzaldehyde) with 100% selectivity from the oxidation of benzyl alcohol (Table 1, entry 1). Interestingly, active aryl secondary alcohol, 1-phenylethanol, was also oxidized to acetophenone in 94% with 100% selectivity (Table 1, entry 2). Surprisingly, electron donating substituents such as methoxy (OCH_3) or chloro (Cl) attached aromatic alcohols (4-methoxy acetophenone or 4-chloro acetophenone) also worked well (Table 1, entries 3 and 4). The oxidation of 4-methoxy acetophenone by Ru/HHP affords the corresponding ketone in good 85% yield with 94% selectivity (Table 1, entry 3). Similarly, 79% of 1-(4-chlorophenyl)ethanone was obtained from the oxidation of 4-chloro acetophenone (Table 1, entry 4). The 2-naphthyl ethanol was oxidized to 2-acetylnapthalene in good yield (98%) with 100% selectivity (Table 1, entry 5). It was found that 1-indanol was transformed to 1-indanone in 69% yield after 24 h with 88% selectivity (Table 1, entry 5). The oxidation of 4-nitrobenzyl alcohol yielded 91% of 4-nitro benzaldehyde with 96% selectivity (Table 1, entry 6).

Most of the Ru catalysts are often found to be less active towards the oxidation of aliphatic alcohols. The present Ru/HHP was found to be able to oxidize the aliphatic alcohols to the corresponding aldehydes effectively. Both less reactive 1-octanol and 2-octanol were readily transformed into 1-octanone (79% yield, 98% selectivity) and 2-octanone (71% yield, 100% selectivity), respectively, without any over-oxidation (Table 1, entries 8 and 9). Worth mentioning is that the sterically hindered alcohol, DL-isoborneol, was efficiently transformed into the corresponding ketone (Table 1, entry 10). More interestingly, heterocyclic alcohol, 2-furyl ethanol, was also oxidized by Ru/HHP to yield 2-acetyl furan in moderate yield (69%).

The yield of the present Ru/HHP system is better or comparable to the best MNPs-supported heterogeneous nanocatalysts Ru/GNS [13], V_2O_5 [39] (79% of benzaldehyde), RuNPs/CNFs [10], Ru/TiO_2 [40] (85% of 2a under O_2/Ar atm), Ru/Al_2O_3 [41] and Ru-substituted silicotungstate [42] (obtained 36% of benzaldehyde under O_2 atmosphere after 120 h). Apart from the comparison, some of the reported catalysts (Ru/GNS and RuNPs/CNFs) were utilized as catalyst (instead of Ru/HHP) for the oxidation of benzyl alcohol under the present optimized conditions. It was found that the Ru/HHP was better (98% of benzaldehyde) when compared to Ru/GNS and RuNPs/CNFs.

3. Ni/HHP Catalyzed *aza*-Michael Reaction

3-1. Optimization of Reaction Conditions

The *aza*-Michael reaction is one of the important transformations in catalysis. The *aza*-adducts are key materials in pharmaceuticals and fine chemicals [14]. Initially, reaction conditions were optimized. In the absence of Ni/HHP, the reaction of 1-phenylpiperazine with acrylonitrile gave moderate yield of the desired product (3-(4-phenylpiperazin-1-yl)propanenitrile) even after longer reaction time. It was found that the reaction can be carried under solvent-free conditions; however, the reaction requires longer reaction time. The rate of the reaction was very fast when the reaction was stirred in acetonitrile. With 2 mg of Ni/HHP, the reaction of 1-phenylpiperazine with acrylonitrile gave an excellent 99% yield of 3-(4-phenylpiperazin-1-yl)propanenitrile. Interestingly, the Ni/HHP system achieved maximum yield of 3-(4-phenylpiperazin-1-yl)propanenitrile even at room temperature (27 °C). The present system could be adapted to transform a higher amount of reactants (2 mmol). A better yield of 99% (3-(4-phenylpiperazin-1-yl)propanenitrile) was obtained when the reaction was performed under solvent-free conditions. The Ni/HHP was active even at room temperature (25 °C) and low amount of catalyst (2 mg of Ni/HHP).

3-2. Scope Extension

The scope of the catalytic system was further studied. Under the adopted reaction conditions, the present Ni/HHP system gave an excellent 99% yield of the desired *aza*-adduct 3-(4-phenylpiperazin-1-yl)propanenitrile with 100% selectivity (Table 2, entry 1). Similarly, in the presence of 2 mg of Ni/HHP, acrylonitrile reacted effectively with various amines (pyrrolidine, piperidine or benzylamine) to yield the corresponding *aza*-adducts in excellent yields with 100% selectivity (Table 2, entries 1-4). Reaction of acrylonitrile and pyrrolidine yielded 3-(pyrrolidin-1-yl)propanenitrile in 98% with 100 selectivity (Table 2, entry 2). An excellent yield of 98% with 100% selectivity of 3-(piperidin-1-yl)propanenitrile was afforded by the Ni/HHP catalyzed reaction of acrylonitrile and piperidine (Table 2, entry 3). In the presence of 2 mg of Ni/HHP, 2 mmol of benzylamine was reacted with 4 mmol of acrylonitrile to obtain 3,3′-(benzylazanediyl)dipropanenitrile in 95% with 100 selectivity (Table 2, entry 4). Methyl acrylate was allowed to react with morpholine and 1-phenylpiperazine to yield methyl 3-morpholinopropanoate (94%) and methyl 3-(4-phenylpiperazin-1-yl) propanoate (96%), respectively (Table 2, entries 5 and 6). Similarly, 91% of ethyl 3-(4-phenylpiperazin-1-yl)propanoate was obtained by the reaction between 1-phenylpiperazine and ethyl acrylate (Table 2, entry 7). The reaction of morpholine and ethyl acrylate in the presence of 2 mg of Ni/HHP affords 93% of ethyl 3-morpholinopropanoate (Table 2, entry 8). The catalytic activity of Ni/HHP in terms of yield is comparable with some of the best heterogeneous nanocatalysts including CuO/GNS [14], Cu/CNFs [10] and nano-CuO [43].

Table 2. *aza*-Michael reaction of amines with *α,β*-unsaturated compound catalyzed by Ni/HHP[a]

Entry	Amine	*α,β*-Unsaturated compound	Product	GC data (%)		
				Conversion	Selectivity	Yield
1	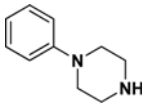		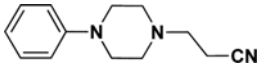	99	100	99
2			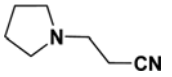	98	100	98
3			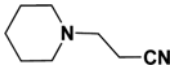	97	100	97
4[e]	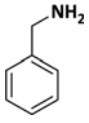		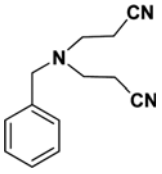	95	100	95
5		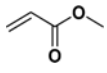	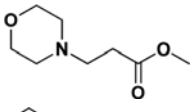	94	100	94
6	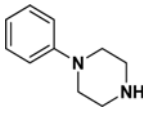	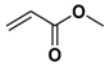	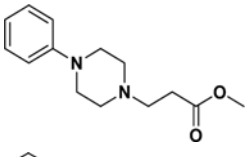	98	98	96
7	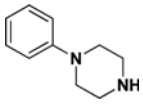	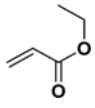	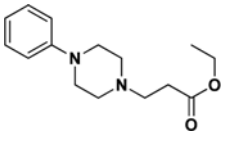	91	100	91
8		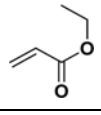	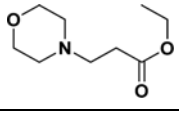	93	100	93

[a]Reaction conditions: amine (2.0 mmol), acrylonitrile (2.0 mmol), Ni/HHP (2 mg), acetonitrile (4 mL), air atmosphere, 1 h, 27 °C
[e]4 mmol of acrylonitrile was used

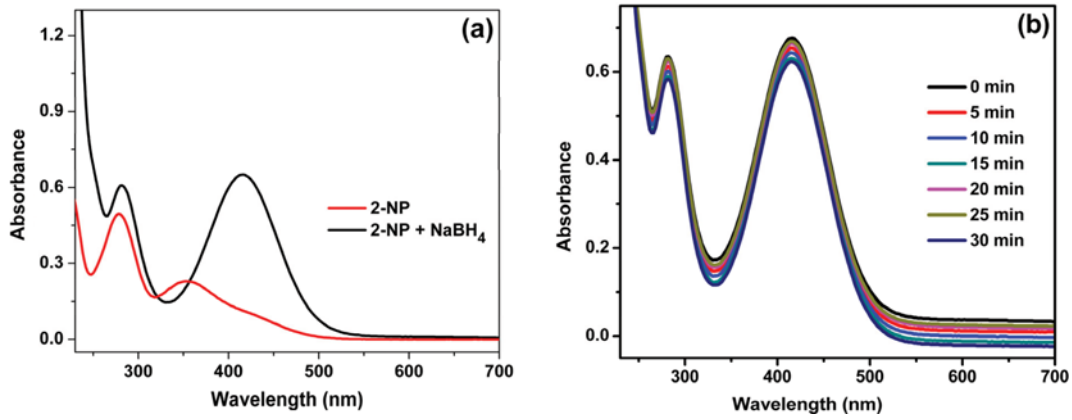

Fig. 5. (a) UV-vis spectra of 2-NP before and after adding $NaBH_4$ solution and (b) the reduction of 2-NP in the presence of pure human hair recorded every 5 min.

4. Reduction of 2-NP by Ru/HHP and Ni/HHP Catalysts

Due to mutagenesis, hepatotoxicity and carcinogenesis, 2-nitrophenol (2-NP) has been listed on the "Priority Pollutions List" of the U.S. Environmental Protection Agency [44,45]. The 2-NP can

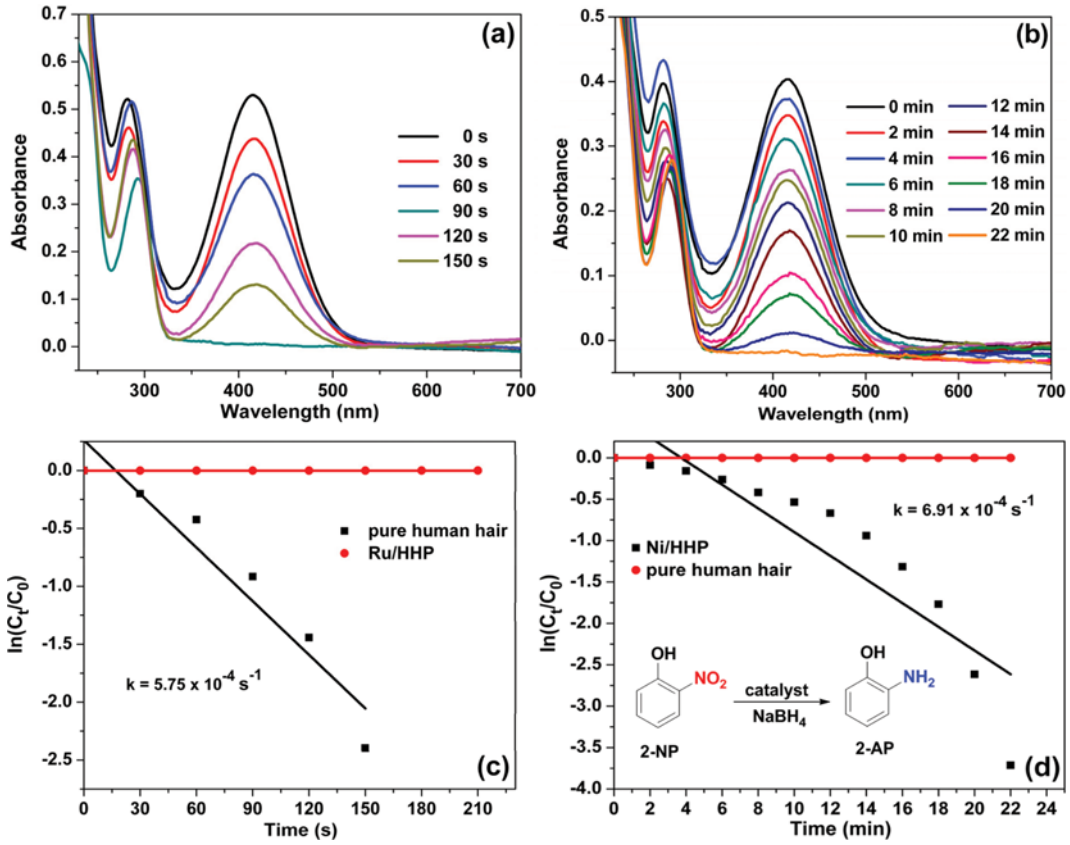

Fig. 6. UV-vis spectra of the reduction of 2-NP in the presence of (a) Ru/HHP and (b) Ni/HHP recorded at particular time intervals. Plots of $\ln[C_t/C_0]$ *versus* reaction time for the reduction of 2-NP with $NaBH_4$ over (c) Ru/HHP and (d) Ni/HHP.

be commonly found in agricultural and industrial wastewaters. Several techniques have been developed for the degradation of 2-NP; however, the methods are highly expensive. Recently, the catalytic reduction of 2-NP using sodium borohydride ($NaBH_4$) as reducing agent is highly focused. In fact, the method is not only very simple but also the resultant catalytic product 2-aminophenol (2-AP) is helpful and beneficial in various fine chemical industries [46-49]. Hence, the present nanocatalysts were further applied for the reduction of 2-NP using $NaBH_4$ as reducing argent.

The reduction of 2-NP to 2-AP is a simple and steady process, but in the absence of catalysts, the reaction is kinetically highly restricted. Blank reactions were carried out to prove the above statement (Fig. 5). Fig. 5(a) shows the UV-vis spectra of 2-NP before and after adding aqueous $NaBH_4$ solution. The pure 2-NP showed a broad band at ~350 nm. Upon the addition of $NaBH_4$ solution, the peak was red-shifted from 350 nm to 416 nm due to the formation of 2-nitrophenolate ions (Fig. 5(a)) [44]. In the absence of catalysts, the peak at 416 nm remained unchanged even after a couple of days (Fig. S3 in Supporting Information). Prior to using Ni/HHP and Ru/HHP as catalysts, initially, e-HHP was employed as catalyst for the reduction of 2-NP. Despite its exceptional elemental composition, the e-HHP was found to be inefficient for the reduction of 2-NP. In the presence of e-HHP, the adsorption peak at 400 nm remained unaltered even after 30 min (Fig. 5(b)). Interestingly, the peak intensity at 416 nm was noticed to be rapidly decreased with the time in the presence of catalysts (Ni/HHP and Ru/HHP). Fig. 6(a) and 6(b) show the UV-Vis absorption spectra of the reduction of 2-NP in the presence of Ru/HHP and Ni/HHP. A small amount of Ni/HHP (2.5 mg) and Ru/HHP (0.5 mg) was enough for the complete reduction of 2-NP with faster reaction rate. For the complete reduction of 2-NP to 2-AP, 0.5 mg of Ru/HHP was found to be enough. The time required for the complete reduction of 2-NP by Ru/HHP was only 150 s. Similarly, a small amount of Ni/HPP (2.5 mg) was determined to be sufficient for the complete reduction of 2-NP (Fig. 6(b)).

Further, reaction kinetics was studied by using the time-dependent absorption spectra. The reaction rate is assumed to be independent of $NaBH_4$ concentration. Similarly, since the e-HHP was found to be inactive for the reduction of 2-NP, the 2-NP adsorption on e-HHP can be ignored. To find the reaction order, four-to-five consecutive data were chosen and linear correlation between $\ln(C_t/C_0)$ and time was obtained (Fig. S4 in Supporting Information). The result confirms that the present catalytic systems follow the pseudo-first-order reaction kinetics. Fig. 6(c) and 6(d) demonstrate the linear correlation between $\ln(C_t/C_0)$ and time at 295 K. The kinetic reaction rate constants (k_{app}) were calculated from the slope of the $\ln(C_t/C_0)$ *versus* time liner curve. The best k_{app} values of 6.91×10^{-4} s^{-1} (by Ni/HHP) and 5.75×10^{-2} s^{-1} (by Ru/HHP) were estimated. The k_{app} values of the present systems are comparable to the previous findings in the literature for the reduction of 2-NP including Ag-Au-rGO nanocomposites ($k_{app}=3.47\times10^{-3}$ s^{-1}) [44], Ni/MC-750 ($k_{app}=6.26\times10^{-3}$ s^{-1}) [45], Ni-RGO ($k_{app}=1.8\times10^{-3}$ s^{-1})

[46], and Pt-Au-pNDs/RGOs (k_{app}=3.8×10^{-3} s^{-1}) [47]. The good catalytic performance of Ni/HHP and Ru/HHP is mainly due to small nanoparticles size, uniform distribution of NPs on e-HHP, strong metal-support interaction. The polyatomic nature of the Ru/HHP and Ni/HHP was also one of the main reasons for the better catalytic performance.

5. Proposed Mechanism

5-1. Ru/HHP Catalyzed Oxidation of Alcohols

Based on the experimental results obtained, we conclude that Ru=O species is an active intermediate for the effective oxidation of alcohols. At first, Ru nanoparticles form Ru=O species with the help of atmospheric oxygen. In fact, the reaction worked well under only air atmosphere but not under inert atmosphere. Subsequently, the formed Ru=O species assisted the formation of benzaldehyde from benzylalcohol. Finally, the Ru/HHP was regenerated for the further use.

5-2. Ni/HHP-catalyzed *aza*-Michael Reaction

The possible mechanism has been proposed for the Ni/HHP-catalyzed *aza*-Michael reaction of amine with acrylonitrile. The mechanism has been proposed based on the results obtained. The piperidine and acrylonitrile act as a Michael donor and acceptor, respectively. In the first step, piperidine is adsorbed on the Ni/HHP, and the attraction between Ni and hydrogen attached to the amine makes the N-H bond weaker and simultaneously enhances the nucleophilicity of the nitrogen for the addition to electron-deficient alkenes. Secondly, the attracted piperidine undergoes reaction with acrylonitrile to form *aza*-Michael adduct. Finally, the catalytic cycle is completed by desorption of the product.

5-3. Catalytic Reduction of 2-NP

In the reduction process, BH_4^- and nitro groups act as donor and acceptor groups respectively. The reduction of 2-NP mainly occurs on the surface of catalyst. At first, nitrophenolate ion adsorbs on the surface of catalysts and generates active hydrogen atoms. During the process, NPs acts as an electronic relay system and accelerates the electron transfer from BH_4^- to nitro groups and the system subsequently gives 2-NP.

6. Heterogeneity Test

Heterogeneous nature of the Ni/HHP and Ru/HHP was tested. To check the heterogeneity of Ru/HHP for the oxidation reaction, a hot filtration test was performed. After 9 h of the reaction (oxidation of benzyl alcohol by Ru/HHP under optimized reaction conditions), the Ru/HHP was separated out from the reaction mixture by a simple centrifugation and the GC yield of benzaldehyde was determined to be 39%. Then the filtrate (Ru/HHP free) was continued stirring for another 15 h and the progress of the reaction monitored at 3 h intervals (Fig. 7(d)). No further conversion occurred after the Ru/HHP removal, which shows the oxidation of reaction occurred only in the presence of Ru/HHP. Further, the heterogeneous nature of Ni/HHP for *aza*-Michael reaction was checked. After the reaction, the Ni/HHP was removed by centrifugation and the Ni content in the filtrate was checked by ICP-MS. The resulting showed there was no Ni content in the filtrate, which

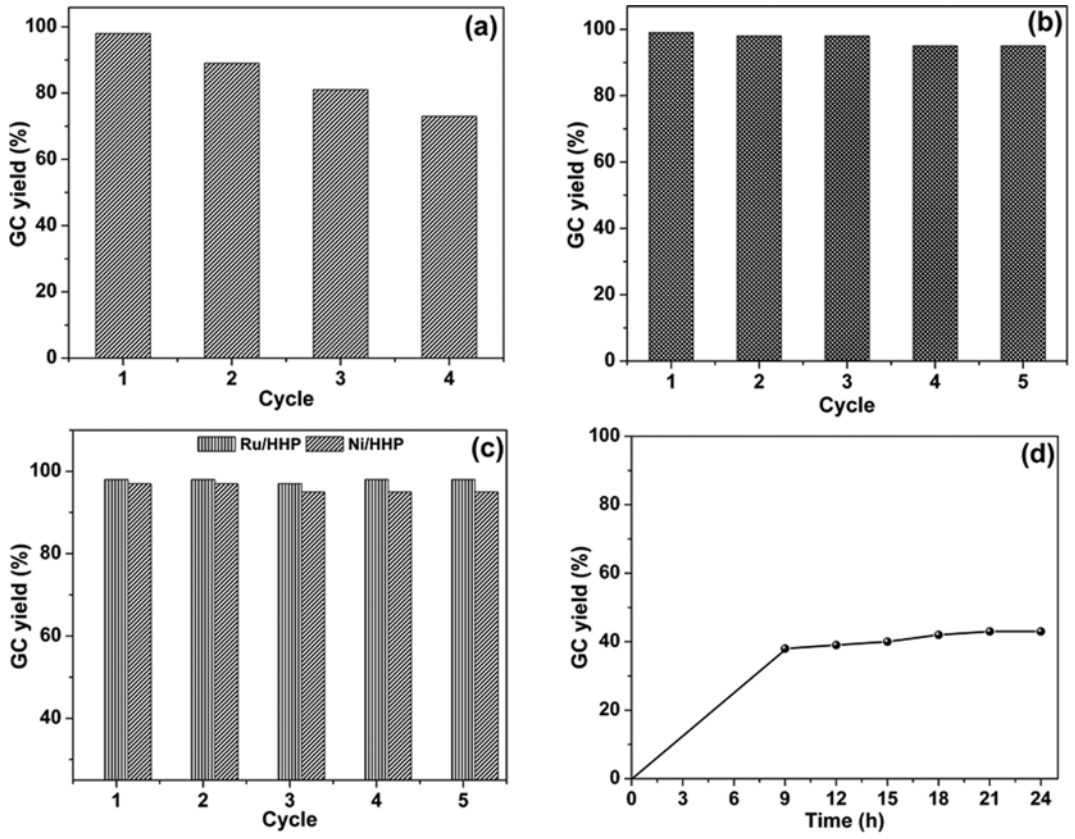

Fig. 7. Reusability of (a) Ru/HHP for oxidation of benzyl alcohol, (b) Ni/HHP for *aza*-Michael reaction, (c) Ru/HHP and Ni/HHP for reduction of 2-NP, and (d) heterogeneity test for Ru/HHP-catalyzed oxidation of benzyl alcohol.

confirmed the heterogeneous nature of the Ni/HHP. Similarly, the metal content of Ni in Ni/HHP (after 5th use) and Ru in Ru/HHP (after 5th use) were found to be almost same with the fresh catalysts. The results show the catalysts are highly stable and heterogeneous.

7. Reusability Test

Recovery and reusability of heterogeneous nanocatalysts are the important advantages, which make them economically feasible. Reusability test was performed for Ru/HHP and Ni/HHP (Fig. 7). The results confirmed that the catalysts are reusable at least for four cycles without significant loss in catalytic activity. After the first cycle, the catalysts were recovered by a simple centrifugation and were washed with diethyl ether and air dried. Then the dried catalyst was reused for further cycles. In the oxidation of benzyl alcohol, at 4th cycle, the Ru/HHP gave good 73% yield of benzaldehyde with 100% selectivity. Similarly, the Ni/HHP affords an excellent yield of 99%, 98%, 95% and 96% of 3-(piperidin-1-yl)propanenitrile at 2nd, 3rd, 4th and 5th cycles. The selectivity of the Ni/HHP was determined to be 100%. Both Ni/HHP and Ru/HHP can be reused at least for five cycles. At 5th cycle, the Ru/HHP gave an excellent yield of 97% of 2-AP. Similarly, the Ni/HHP gave an excellent yield of 98%, 97%, 96%, 96% and 97% at 2nd, 3rd, 4th and 5th cycles, respectively.

CONCLUSIONS

Ru- and Ni-based human hair nanocomposites (Ni/HHP and Ru/HHP) were successfully prepared. The physicochemical properties of resultant Ni/HHP and Ru/HHP were found to be excellent. The merit of the Ni/HHP and Ru/HHP was realized from its excellent catalytic activity towards (i) oxidation of alcohols, (ii) *aza*-Michael reaction, and (iii) reduction of 2-NP. The Ni/HHP and Ru/HH are reusable and heterogeneous. Overall, non-toxic, availability, economical and excellent activity would make human hair nanocomposites one of the alternate choices for the existing biomass derived catalysts.

ACKNOWLEDGEMENTS

This study was supported by the Konkuk University KU research professor program.

SUPPORTING INFORMATION

Additional information as noted in the text. This information is available via the Internet at http://www.springer.com/chemistry/journal/11814.

REFERENCES

1. D. Astruc, F. Lu and J. R. Aranzaes, *Angew. Chem. Int. Ed.*, **44**, 7852 (2005).
2. J. M. Campelo, D. Luna, R. Luque, J. M. Marinas and A. A. Romero, *ChemSusChem.*, **2**, 18 (2005).
3. Y. Zhang, G. Xiong, S. Sheng and W. Yang, *Catal. Today*, **63**, 517 (2000).
4. J. S. Hoon, J. Y. Park, C. K. Tsung, Y. Yamada, P. Yang and G. A. Somorjai, *Nat. Mater.*, **8**, 126 (2009).
5. T. E. James, S. L. Hemmingson and C. T. Campbell, *ACS Catal.*, **5**, 5673 (2015).
6. X. Yujia, F. Zhang, P. Liu, F. Hao and H. Luo, *J. Mol. Catal. A-Chem.*, **386**, 95 (2014).
7. C. W. Chiang, A. Wang and C. Y. Mou, *Catal. Today*, **117**, 220 (2006).
8. M. Gopiraman, S. G. Babu, Z. Khatri, W. Kai, Y. A. Kim, M. Endo, R. Karvembu and I. S. Kim, *Carbon*, **62**, 135 (2013).
9. S. W. Pattinson, A. H. Windle and K. K. K. Koziol, *Mater. Lett.*, **93**, 404 (2013).
10. M. Gopiraman, H. Bang, G. Yuan, C. Yin, K. H. Song, J. S. Lee, I. M. Chung, R. Karvembu and I. S. Kim, *Carbohydr. Polym.*, **132**, 554 (2015).
11. Z. Zhuang, S. A. Giles, J. Zheng, G. J. Jenness, S. Caratzoulas, D. G. Vlachos and Y. Yan, *Nat. Commun.*, **7**, 10141 (2015).
12. L. M. Guard, M. M. Beromi, G. W. Brudvig, N. Hazari and D. J. Vinyard, *Angew. Chem. Int. Ed.*, **54**, 13352 (2015).
13. M. Gopiraman, S. G. Babu, Z. Khatri, K. Wei, Y. A. Kim, M. Endo, R. Karvembu and I. S. Kim, *J. Phys. Chem. C*, **117**, 23582 (2013).
14. M. Gopiraman, D. Deng, S. G. Babu, T. Hayashi, R. Karvembu and I. S. Kim, *ACS Sustain. Chem. Eng.*, **3**, 2478 (2015).
15. M. Gopiraman, R. Karvembu and I. S. Kim, *ACS Catal.*, **4**, 2118 (2014).
16. M. Gopiraman, H. Bang, S. G. Babu, K. Wei, R. Karvembu and I. S. Kim, *Catal. Sci. Technol.*, **4**, 2099 (2014).
17. M. Gopiraman, S. G. Babu, R. Karvembu and I. S. Kim, *Appl. Catal. A-Gen.*, **484**, 84 (2014).
18. M. Gopiraman, S. G. Babu, Z. Khatri, K. Wei, E. Morinobu, R. Karvembu and I. S. Kim, *Catal. Sci. Techol.*, **3**, 1485 (2013).
19. S. G. Babu, M. Gopiraman, D. Deng, K. Wei, R. Karvembu and I. S. Kim, *Chem. Eng. J.*, **300**, 146 (2016).
20. M. Gopiraman, S. G. Babu, Z. Khatri, B. S. Kim, K. Wei, R. Karvembu and I. S. Kim, *React. Kinet. Mech. Cat.*, **115**, 759 (2015).
21. M. Kaushik and A. Moores, *Green Chem.*, **18**, 622 (2016).
22. X. Lu and S. Cui, *Bioresour. Technol.*, **101**, 4703 (2010).
23. K. Deplanche, J. A. Bennett, I. P. Mikheenko, J. Omajali, A. S. Wells, R. E. Meadows, J. Wood and J. E. Macaskie, *Appl. Catal. B.*, **147**, 651 (2014).
24. R. B. Nasir Baig, M. N. Nadagouda and R. S. Varma, *Green Chem.*, **16**, 2122 (2014).
25. A. Brito, F. Garcia, C. Alvarez, R. Arvelo, J. L. G. Fierro and C. Diaz, *Ind. Eng. Chem. Res.*, **43**, 1659 (2004).
26. M. Nasrollahzadeh, A. Azarian, M. Maham and A. Ehsani, *J. Ind. Eng. Chem.*, **21**, 746 (2015).
27. N. Edayadulla, N. Basavegowda and Y. R. Lee, *J. Ind. Eng. Chem.*, **21**, 1365 (2015).
28. K. Anand, R. M. Gengan, A. Phulukdaree and A. Chuturgoon, *J. Ind. Eng. Chem.*, **21**, 1105 (2015).
29. A. Gupta, *J. Waste Manage.*, **2014**, 1 (2014).
30. R. C. Clay, K. Cook and J. I. Routh, *J. Am. Chem. Soc.*, **62**, 2709 (1940).
31. H. Lee, K. Noh, S. Lee, I. Kwon, D. Han, I. Lee and Y. Hwang, *Tissue Eng. Regen. Med.*, **11**, 255 (2014).
32. S. D. Haveli, P. Walter, G. Patriarche, J. Ayache, J. Castaing, E. V.

Elslande, G. Tsoucaris, P. A. Wang and H. B. Kagan, *Nano Lett.*, **12**, 6212 (2012).
33. P. Walter, E. Welcomme, P. Hallegot, N. J. Zaluzec, C. Deeb, J. Castaing, P. Veyssiere, R. Breniaux, J. L. Leveque and G. Tsoucaris, *Nano Lett.*, **6**, 2215 (2006).
34. D. Deng, M. Gopiraman, S. H. Kim, I. M. Chung and I. S. Kim, *ACS Sustainable Chem. Eng.*, **4**, 5409 (2016).
35. N. Akira, A. Makoto, T. Keiji and F. Toshihiro, *Biol. Pharm. Bull.*, **25**, 569 (2002).
36. A. Idris, R. Vijayaraghavan, U. A. Rana, D. Fredericks, A. F. Pattia and D. R. MacFarlanea, *Green Chem.*, **15**, 525 (2013).
37. N. T. B. Hien, H. Y. Kim, M. Jeon, J. H. Lee, M. Ridwan, R. Tamarany and C. W. Yoon, *Materials*, **8**, 3442 (2015).
38. G. P. Jin, Y. F. Ding, P. P. Zheng, *J. Power Sources*, **166**, 80 (2007).
39. S. Velusamy and T. Punniyamurthy, *Org. Lett.*, **6**, 217 (2004).
40. A. Kockritz, M. Sebek, A. Dittmar, J. Radnik, A. Bruckner, U. Bentrup, M. M. Pohla, H. Hugl and W. Magerlein, *J. Mol. Catal. A-Chem.*, **246**, 85 (2006).
41. A. Zsigmond, F. Notheisz, G. Csjernyik and J. E. Backvall, *Top Catal.*, **19**, 119 (2002).
42. K. Yamaguchi and N. Mizuno, *New J. Chem.*, **26**, 972 (2002).
43. M. L. Kantam, S. Laha, J. Yadav and S. Jha, *Tetrahedron Lett.*, **50**, 4467 (2009).
44. M. Zhenye, W. Rujun, H. Qiaorong, C. Rizhi and G. Zhenggui, *Korean J. Chem. Eng.*, **28**, 717 (2011).
45. D. Yan and C. Rizhi, *Korean J. Chem. Eng.*, **32**, 1759 (2015).
46. K. Hareesh, R. P. Joshi, D. V. Sunitha, V. N. Bhoraskar and S. D. Dhole, *Appl. Surf. Sci.*, **389**, 1050 (2016).
47. Y. Yang, Y. Ren, C. Sun and S. Hao, *Green Chem.*, **16**, 2273 (2014).
48. Y. Tian, Y. Liu, F. Pang, F. Wang and X. Zhang, *Colloids Surfaces A: Physicochem. Eng. Aspects*, **464**, 96 (2015).
49. J. J. Lv, A. J. Wang, X. Ma, R. Y. Xiang, J. R. Chen and J. J. Feng, *J. Mater. Chem. A*, **3**, 290 (2015).

Supporting Information

Multifunctional human-hair nanocomposites for oxidation of alcohols, *aza*-Michael reactions and reduction of 2-nitrophenol

Mayakrishnan Gopiraman and Ill-Min Chung[†]

Department of Applied Bioscience, College of Life & Environment Science, Konkuk University,
120, Neungdong-ro, Gwangjin-gu, Seoul 05029, Korea
(*Received 24 February 2017 • accepted 12 April 2017*)

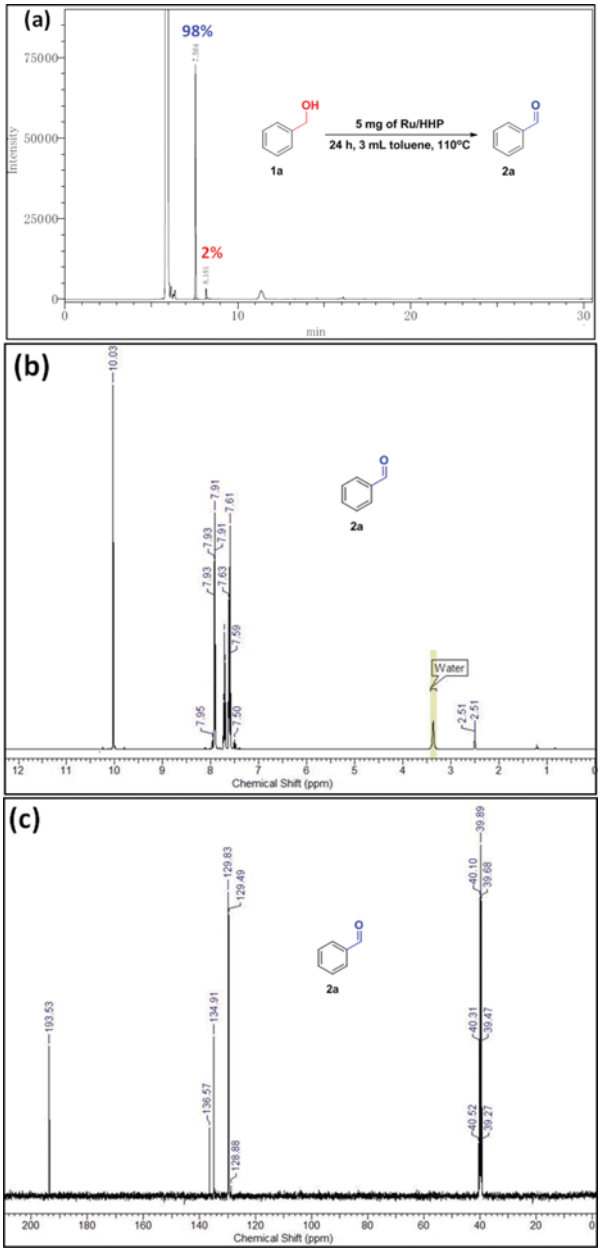

Fig. S1. (a) GC chromatogram, (b) ^{1}H NMR spectrum and (c) ^{13}C NMR spectrum of 2a.

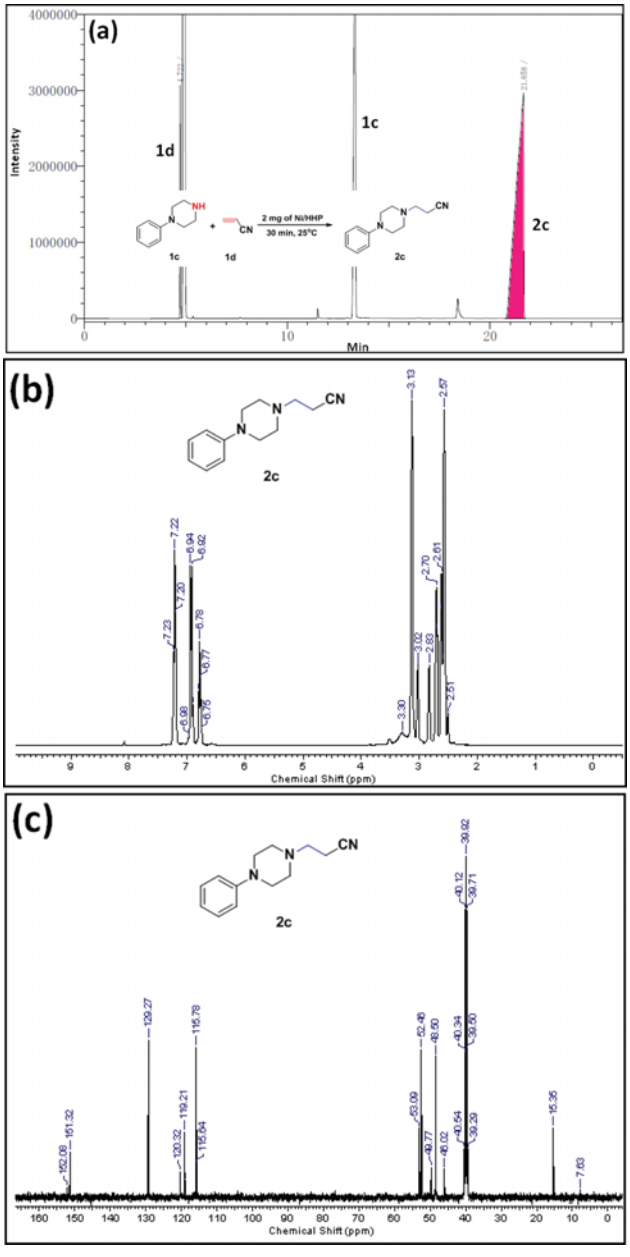

Fig. S2. (a) GC chromatogram, (b) ^{1}H NMR spectrum and (c) ^{13}C NMR spectrum of 2c.

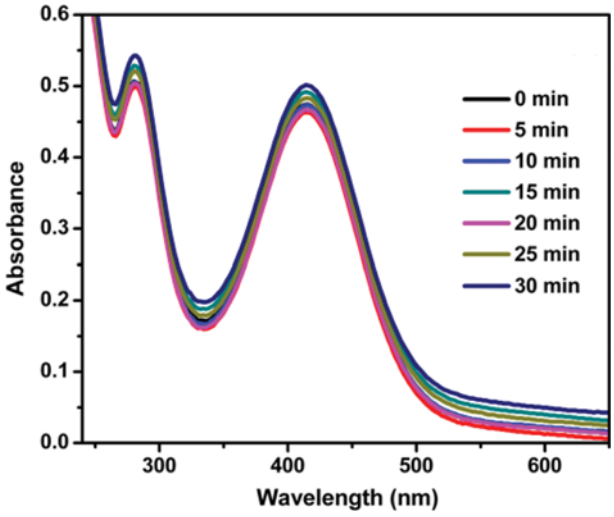

Fig. S3. UV-vis spectra of the reduction of 4-NP in the presence of $NaBH_4$ recorded every 5 min.

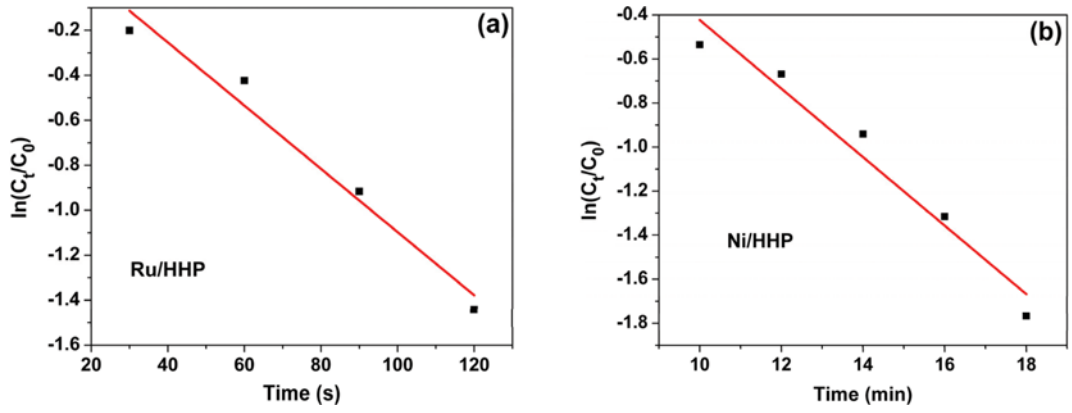

Fig. S4. Plots of $\ln[C_t/C_0]$ *versus* reaction time for the reduction of 2-NP with $NaBH_4$ over (a) Ru/HHP and (b) Ni/HHP.

GC chromatogram, ^{1}H and ^{13}C NMR spectra